Proceedings World Geothermal Congress 2026
Calgary, Canada, June 8 – 11, 2026

Efficient Modelling and Risk Assessment for Aquifer Thermal Energy Storage in Fractured Rocks: How uncertainty quantification can convince decision makers

Tas L[1]*, Jacquemyn C[2] , Jackson MD[2], Bahlali ML[2] and Hermans T[1]
Laboratory for Applied Geology and Hydrogeology, Department of Geology, Ghent University, Belgium[1]*,
Novel Reservoir Modelling and Simulation Group, Department of Earth Science Engineering, Imperial College London, UK[2]
luka.tas@ugent.be

Keywords: fracture network, stochastic analysis, LT-ATES, uncertainty analysis, field data

INTRODUCTION

Seasonal aquifer thermal energy storage (ATES) in groundwater is a promising alternative to heat and cool buildings sustainably. Essentially, excess heat and cold is stored in the subsurface and recovered when needed. Currently, most operational systems are located in the Netherlands (Fleuchaus et al., 2018). There, storage aquifers are predominantly sandy and homogeneous allowing to store and recover thermal energy efficiently without substantial uncertainty. So far, the ATES expertise has been limited to this kind of setting and more complex storage aquifers remain largely untapped. The currently rising energy cost and government incentives to invest in local and sustainable energy resources, incentivizes to explore complex hydrogeological settings. This encourages ATES developments outside the Netherlands, in storage aquifers beyond the traditional sandy target. Fractured rock reservoirs are such a strategic, yet highly challenging target. The unknown and heterogeneous presence of preferential flow paths propagates into uncertainty about thermal recovery efficiency. The currently accepted method for feasibility studies fails to address this uncertainty making it difficult to correctly inform decision-makers about project feasibility.

To address this and move ATES developments forward, this study introduces an approach to model ATES systems in fractured rocks. To mimic the workflow of a consulting company in case of a lack of data, several distinct conceptual models are analysed in which fractures are explicitly represented (in a simplified way). For this study, the concepts are based on the fractured basement rock in Brussels (Belgium). Each conceptual model represents a different degree of connectivity between the wells and the surrounding rock, as well as between the cold and warm wells. Conceptual models are selected for further analysis based on their capability to represent the well connectivity observed in exploratory wells. To allow for uncertainty quantification, a broad prior uncertainty range is then included on subsurface parameters of the storage aquifer. A short-term (fluorescence) tracer test and long-term ATES system are simulated. Once the uncertainty range is validated based on the available tracer test data, statistical modelling will be used to find a direct relationship between data and prediction. As such, this study aims to make a long term ATES prediction that is constrained by short term field data with a quantification of the uncertainty on the prediction.

1 METHODS & RESULTS

1.1 Conceptual Models

Before randomly generating models with different subsurface parameters for uncertainty quantification, several conceptual models with a distinct connectivity are evaluated. This approach aims to first better understand the behaviour of a fractured rock reservoir in response to injection and abstraction.

The fractured basement rock in Belgium serves as a base case in this study and an extensive review of available data has been conducted. This includes data from pump-injection tests, flowmeter logs, borehole images, fluorescence tracer tests, borehole diameter logging, operational ATES systems, public databases, lithology logging, and more general regional (hydro)geological studies. In short, these studies reported the following characteristics: (I) the bedrock is composed of low-grade metamorphic quartzites and phyllites, and is directly overlain by Cretaceous chalk deposits or a clayey aquiclude, (II) there is a regional natural groundwater flow from SE to NW, (III) on average 2 to 5 distinct highly fractured productive zones (each 1 to 10 m in thickness) are crossed when drilling a well, (IV) groundwater flow is mainly controlled by fractures, (V) there is no decisive knowledge of fracture orientation but a dip angle from 50° to 90° seems prevalent, (VI) aquifer flow rates are estimated to be 10-150 m^3/h.

Even though substantial subsurface information is available, its practical use remains limited because the spatial correlation scale is smaller than the average well spacing of an ATES doublet. Due to the unpredictable heterogeneous nature of the basement rock, this study therefore rather focuses on representing larger scale connectivity features. Several conceptual models are tested with a specific connectivity between the wells and the surrounding rock, as well as between the cold and warm wells. Specifically, the 3D model encompasses an area of 1 by 1 km around the centre of an ATES doublet which is placed perpendicular to the natural hydraulic gradient. For this study the well spacing is 60 m and well screens range from 84 m to 160 m deep. The overburden deposits are 84 m thick. Below, the basement rock contains a number of distinct fracture zones. The bottom of the model is 250 m deep, ensuring a sufficient distance from the bottom of the wells. Fractures are explicitly modelled. To limit computational time and to represent different degrees of connectivity, their extent is bounded by cylindrical geometries which have a height equal to the thickness of the fracture zone. Depending on the radius and centerpoint of the cylinder, a different connectivity of the wells is represented (Fig. 1). Two fracture sets are modelled within each cylinder. Additionally, larger fractures, crosscutting the entire model domain can be added to represent vertical connectivity between different fracture zones. In this study, all fracture widths are set to 1 m, which is larger than in reality but suffices to capture the influence of preferential flow paths. Rather than trying to capture the full fracture network, as done in previous studies of for instance Jin et al. (2025), it allows focusing on connectivity that matters with lower computational cost. For flexibility, a script is written in Coreform Cubit for surface-based modelling (after Jacquemyn et al., 2019) in which the properties of the wells (diameter, depth, screen length, location), the fracture zones (depth, thickness, number), the fracture cylinders (radius, centerpoint) and the fracture planes (width, dip angle, strike angle, density) can be set. This allows to efficiently generate a large number of alternative conceptual modes. As such, the well connectivity modelling strategy can also be applied to other locations in Brussels, apart from the location of which the field data will be used in this study. Once the surfaces have been defined, the initial model and tetrahedral mesh is generated.

For an ATES feasibility study in such a complex setting, usually 1 or 2 test wells are drilled. Based on the information during drilling and initial pump-injection (and potentially) tracer tests, the conceptual models can be evaluated. If they reproduce the hydrogeological behaviour of the aquifer observed during field tests, the concepts should be selected for further analysis with uncertainty quantification. For this study, tracer test data from a study site in Brussels is available. The tracer test lasted 11 days. After five hours of pump-injection (57.5 m^3/h) a steady state was reached and 5 kg of fluorescence tracer was added over the course of 10 minutes.

The IC-FERST simulator is used to model groundwater flow and (heat) transport (https://multifluids.github.io/). Unlike more traditional modelling software such as MODFLOW, IC-FERST uses a surface-based representation of geological heterogeneity, dynamic mesh optimization, and a DCVFE (double control-volume-finite-element) formulation. This overcomes the computational burden of pillar grids and numerical methods which experience difficulties in modelling neighbouring geological features with highly contrasting subsurface properties. Therefore it is highly suited for complex models with a (simplified) explicit representation of fractures (Salinas et al., 2021).

Fig. 1 shows the results of the tracer experiment and compares it to the simulated model response. For conciseness, a selection is shown of 4 different conceptual model. These 4 models all have a dip angle of 50° for fracture set 1, and 80° for fracture set 2. Each model of the selection has 2 fracture zones in the basement rock. The upper one has a thickness of 2 m and centre depth of 127m, the lower one has a thickness of 4 m and centre depth of 136 m.

In concept 1 there is no direct connection between the injection and extraction wells by preferential flow paths. The injection well directly crosses a fracture in the upper fracture horizon which makes the groundwater transport of the tracer confined by the preferential flow path. As the tracer moves further away, the concentration front becomes more diluted and takes an elongated (hollow) ellipsoid shape. In the lower fracture horizon, the tracer first has to pass through the matrix before reaching the fractures. A cylindrical propagation front therefore precedes the fracture confined transport. At early times, the concentration front is symmetrical around the injection well in both fracture zones, but advection is slower in the lower fracture zone. In the breakthrough curve, the tracer arrival from the 2 distinct fracture zones can be distinguished as two separate peaks. In reality these arrivals would be smoother due to the presence of multiple smaller fractures rather than the large 1 m wide preferential flow paths conceptualized in the model, which explains the difference with the measured field data showing a single peak.

In concept 2, the fracture cylinder includes both injection and extraction wells but the strike angle of all fractures is 110°. This forces the tracer to move through the matrix before arriving at the extraction well, causing a delay in the tracer's first arrival and a trailing part of the breakthrough curve with higher concentration. In both fracture

zones, the tracer first has to pass through the matrix before reaching the fractures, additionally slowing down the tracer. The tracer front at early times is symmetrical in both fracture zones and the advection velocity in both fracture zones is similar. The larger extent of the fractures also causes more tracer to be lost compared to a scenario where the cylinder radius is smaller (while still encompassing both wells).

Concept 3 is equivalent to concept 1, but has additional vertical fractures that are crosscutting the entire model (dip of 80°, strike of 80°). In the upper fracture zone there is now a direct connection by preferential flow paths between the injection and extraction wells. Therefore, the lower fracture zone has only a minor contribution. Almost all tracer transport is constrained by the fracture that is directly crossed by the injection well, up to the point where the crosscutting fractures are reached and the tracer continues to follow this preferential flow path. At that point a large amount of tracer also moves up and down (creating a vertical disc-like shape attached to the elongated ellipsoid). The connection between injection and extraction wells is reflected by the sharp first arrival and narrow peak of the breakthrough curve

Concept 4 is included to illustrate what a 'bad' conceptual model would look like. In the upper fracture zone both wells directly cross the fracture, creating a narrow preferential flow path from injection well straight to extraction well. This results in a very sharp and early tracer arrival. The concentration front is also asymmetric because a strong hydraulic gradient is created towards the extraction well. There is only a minor contribution of the lower fracture zone, where tracer first has to pass through the matrix before it can move through the fractures.

Initially, no recirculation of the tracer was considered. However, even with preliminary subsurface parameter variation, all concepts struggle to capture the tail of the breakthrough curve. Recirculation of the tracer after the initial extraction showed to be indispensable to reproduce the steady arrival of the tracer at later times.

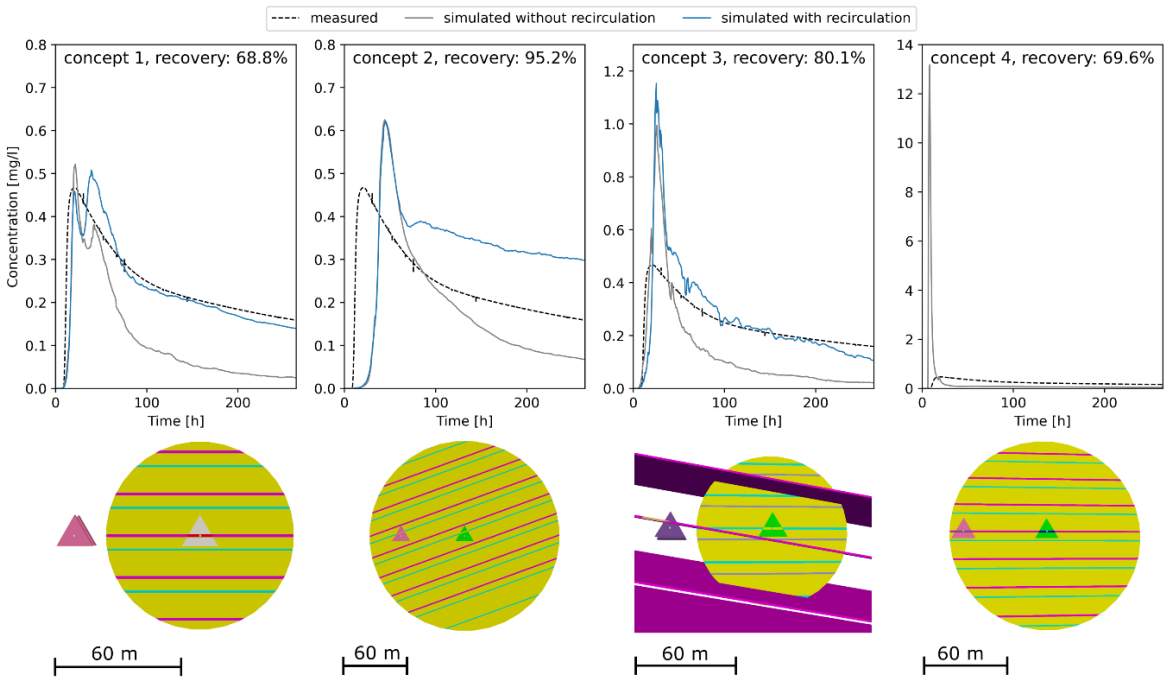


Figure 1. Comparison of the simulated and measured breakthrough curves for four different conceptual models. The recovery percentage corresponds to the recirculation cases (for the first 3 plots). Below, the fracture cylinder geometry, fractures and wells (centre of triangle) are shown for each concept.

1.2 Including Uncertainty in Models

After evaluating variability in conceptual models, uncertainty on subsurface parameters is included. To do this, latin hypercube random sampling from a uniform distribution is used to ensure a good coverage across the multi-dimensional parameter space. Uncertain subsurface parameters include the natural hydraulic gradient (U[25:60] (Pa/m)), basement rock permeability (U[1e-14:1e-13] (m^2)), basement rock porosity (U[0.04:0.08]), fracture zone permeability (U[1e-14:5e-13] (m^2)), fracture zone porosity (U[0.04:0.08]), fracture cylinder permeability (U[1e-12:5e-11] (m^2)), fracture cylinder porosity (U[0.1:0.2]), fracture permeability (U[1e-9:1.2e-7] (m^2)), fracture porosity (U[0.25:0.5]), longitudinal dispersivity (U[0.5:10]) (m), and diffusivity (U[9e-10:10e-10])

(m^2/s). Initially, vertical permeability is set equal to the horizontal permeability, but this could be adjusted in the future. Transverse dispersivity is set to 1/10 of the longitudinal dispersivity.

Conceptual models producing predictions consistent with field data are selected for this further analysis. To test this, the end members of the parameter variation ranges are simulated and compared to field data. For example, Fig. 2 shows that concept 3 will likely be a good candidate for further analysis with Monte Carlo simulations. The simulations show variation in peak height, first arrival time and tailing around the field data. This means that the subsurface parameter variation ranges will likely not be falsified.

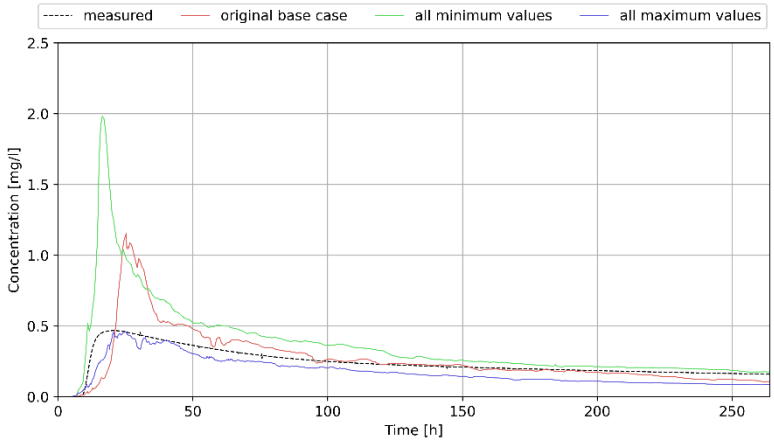


Figure 2. Illustration of the range of variation in model response for the tracer test with concept 3.

To identify most influential parameters, the distance-based global sensitivity analysis (DGSA) method will be used because it has been demonstrated effective and computationally efficient in previous (heat) transport studies (Tas et al., 2025; Zhang et al., 2025). For correct sensitivity analysis approximately 250 to 500 randomly sampled samples will be required. The ensemble of all model realizations is then called the prior distribution.

1.3 From Short to Long Term Predictions

Figure 3 shows the complex storage volume geometry resulting from an ATES simulation with model concept 3. The ATES system operates in 4 seasons with equal duration: heat storage (17 °C), resting period, cold storage (9°C), resting period. The flow rate is 22.6 m^3/h. Fig. 3 highlights the complexity of simulating heat storage in fractured rocks. Heat (/cold) transport is focused along discrete preferential pathways. While the heat moves fast inside the fractures by advection, conduction at the boundaries towards the matrix must also be accurately captured. Therefore small scale processes of tens of centimetres must be simulated in a large model domain of 1 by 1 km. In the fractures, total porosity is larger than effective porosity increasing thermal retardation.

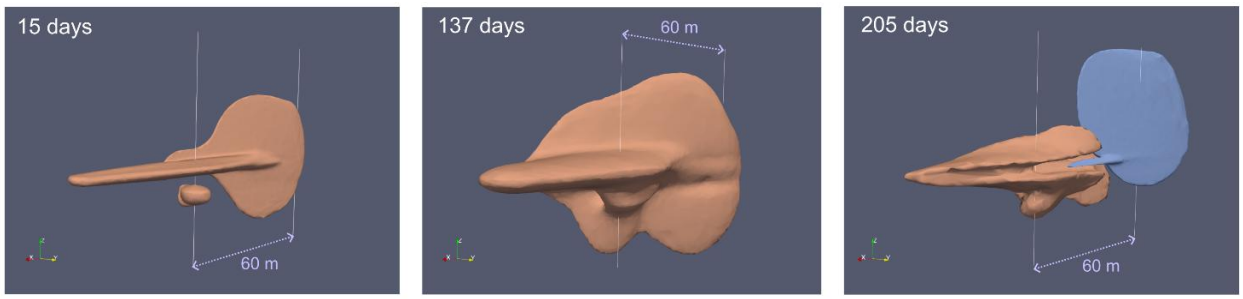


Figure 3. Contour plot of the warm plume (14.5°C contour) and cold plume (11.5 °C contour) propagation.

DGSA will be applied on both the short term tracer test and the long term ATES prediction. In order for the tracer test to be informative about the long term prediction, both should be sensitive to the same parameters. This might be a challenge to overcome when using a solute tracer test as proxy for predicting thermal transport in fractured reservoirs. If sensitivity for field test and long term prediction is similar, a direct relationship between the field data and the model prediction can be found and the relationship can be used to make a prediction of the long term ATES behaviour. This means that the prior distribution of the long term prediction can be refined to a posterior distribution by constraining it with the observed data. The fact that the posterior distribution still has a range of variation and not reflects one single model realization allows for uncertainty quantification determining the probability of reaching a certain thermal recovery efficiency of the ATES system. This approach

is known as Bayesian Evidential Learning (BEL) (Hermans et al., 2019). To find the data-prediction relationship statistical modelling is used combining dimension reduction techniques with statistical/machine learning.

2 DISCUSSION & CONCLUSION

This study evaluates a new approach of modelling a fractured rock aquifer for ATES efficiency predictions. Fractures act as preferential flow paths and are explicitly, yet simplified, modelled in a 3D groundwater flow and (heat) transport model. Rather than focusing on capturing the small scale fracture network, emphasis is on capturing the main connectivity features around the wells. For this study fluorescence tracer test data was available from a study site in Brussels. Different concepts are able to capture different features of the measured breakthrough curve validating the practical use of the well connectivity modelling strategy. With recirculation, concept 1 matches the field observations well. Concept 2 simulates a generally higher tail concentration. Concept 3 precisely captures the first arrival time and showed a prior distribution likely consistent with field data. This study further demonstrates that tracer recirculation, even though at low concentration, is crucial to explain the trailing part of the breakthrough curve measured in the field. Without recirculation only about 35 % of the tracer is recovered in concept 1. With recirculation there is an apparent recovery of 68.8 %, implying that about half of the tracer measured at the abstraction well in the field originates from recirculation. Without subsurface parameter calibration, this well connectivity modelling strategy in a fractured reservoir already provides a better fit compared to a previously calibrated equivalent porous medium model, where the first arrival time matched but where the peak height was 1.6 mg/l and average tail concentration 0.4 mg/l. Concepts 1 and 3 best capture the main features of the measured breakthrough curve and are selected for further analysis. Detailed sensitivity analysis and Bayesian Evidential learning will be applied on both the tracer test and the long term ATES model. In this way we aim to do uncertainty quantification of the ATES efficiency which is crucial for transparent communication of uncertainty related to an investment. The results will be validated with drawdown data from pump-injection tests for the short term prediction and with ATES operational data for the long term prediction.

Acknowledgements

Luka Tas has received funding from FWO for a PhD fellowship (grant number: 1SH0M24N) and for a research stay at the NORMS group at Imperial College London (grant number: V433725N).

REFERENCES

Fleuchaus, P., Godschalk, B., Stober, I., & Blum, P. (2018). Worldwide application of aquifer thermal energy storage – A review. *Renewable and Sustainable Energy Reviews*, *94*, 861-876. https://doi.org/10.1016/j.rser.2018.06.057

Hermans, T., Lesparre, N., De Schepper, G., & Robert, T. (2019). Bayesian evidential learning: A field validation using push-pull tests. *Hydrogeology Journal*, *27*(5), 1661-1672. https://doi.org/10.1007/s10040-019-01962-9

Jacquemyn, C., Jackson, M. D., & Hampson, G. J. (2019). Surface-Based Geological Reservoir Modelling Using Grid-Free NURBS Curves and Surfaces. *Mathematical Geosciences*, *51*(1), 1-28. https://doi.org/10.1007/s11004-018-9764-8

Jin, Y., Ding, Y., Li, C., Qin, Z., & Wang, Q. (2025). Heat recovery efficiency optimization of High-Temperature Aquifer Thermal Energy Storage system in naturally fractured reservoirs: A combined multi-physics modeling and regression prediction method. *Case Studies in Thermal Engineering*, *67*, 105856. https://doi.org/10.1016/j.csite.2025.105856

Salinas, P., Regnier, G., Jacquemyn, C., Pain, C. C., & Jackson, M. D. (2021). Dynamic mesh optimisation for geothermal reservoir modelling. *Geothermics*, *94*, 102089. https://doi.org/10.1016/j.geothermics.2021.102089

Tas, L., Hartog, N., Bloemendal, M., Simpson, D., Robert, T., Thibaut, R., Zhang, L., & Hermans, T. (2025). Efficiency and heat transport processes of low-temperature aquifer thermal energy storage systems: New insights from global sensitivity analyses. *Geothermal Energy*, *13*(1), 2. https://doi.org/10.1186/s40517-024-00326-1

Zhang, L., Mi, Z., Cao, W., Liu, L., Tas, L., & Hermans, T. (2025). Multi-objective optimization of energy efficiency and geomechanical safety in high-temperature aquifer thermal energy storage (HT-ATES) systems based on coupled thermo-hydro-mechanical (THM) analysis. *Energy*, *332*, 137096. https://doi.org/10.1016/j.energy.2025.137096